communications sustainability

A Nature Portfolio journal

Article

https://doi.org/10.1038/s44458-026-00064-4

Soil degradation in Europe is projected to accelerate under changing land use and climate

Mehdi H. Afshar[1,2] ✉, Amirhossein Hassani[3], Pasquale Borrelli[4], Panos Panagos[5], David A. Robinson[6], Dani Or[7] & Nima Shokri[1,2] ✉

Soil degradation threatens food security and environmental sustainability, yet future projections of it are rare. Using projections from 18 global climate models under two Shared Socioeconomic Pathways (SSP2-4.5 and SSP5-8.5) and land-use projections from the Land Use and Climate Across Scales Land Use Change (LUCAS LUC) dataset, we assess future soil vulnerability to degradation by linking a Soil Degradation Proxy (SDP) to climate, land-use, soil characteristics, and socio-economic factors at 7433 observation sites across Europe. We project that by 2071–2100, ~59% of sites may become more vulnerable under the high-emission scenario. Cold forest regions in northern Europe are projected to face increased degradation pressure by ~+0.04SDP. However, some European croplands may improve locally through conversion to secondary lands, reduced human pressures, and natural recovery processes. These regionally specific trends highlight that, while soil degradation remains a major threat, proactive land management can mitigate soil vulnerability under future climate trajectories.

Soil degradation is the persistent decline in the capacity of the soil to support human and other life on Earth[1,2]. This process represents a global challenge that threatens food security, environmental sustainability, and the health of ecosystems that support agricultural productivity, water regulation, and carbon storage[3–5]. The functioning of these and other ecosystems is increasingly threatened by processes, such as soil erosion, nutrient depletion, and loss of soil biodiversity[6–10]. Anthropogenic activities, such as land-use change, management pressure, overgrazing, and pollution, including excessive use of agrochemicals, also contribute to soil degradation[11–13]. Across Europe approximately 62% of soils are affected by at least one degradation process, with about 23% experiencing water erosion rates above 2 tonnes per hectare per year (often used as a tolerable loss benchmark indicating sustained topsoil removal and on-site productivity risk) and over 22% facing nitrogen surpluses exceeding 50 kilograms per hectare (reflecting a nutrient imbalance that raises the risk of leaching and eutrophication)[14].

Climate change contributes to modifying key soil functions[15–17]. Shifts in mean temperature and precipitation patterns can negatively impact the decomposition rate of organic matter[18], reduce soil moisture[19], and increase erosivity[20]. Extreme weather events, such as prolonged droughts or intense rainfall, can further accelerate these processes[15,21]. Additionally, climate change can also influence vegetation cover, which in turn contributes to organic matter loss and increases risks linked with soil degradation processes[22–24].

In addition to climate change, land-use change driven by human activities and climate-related factors significantly alters soil degradation risks[9,25]. Land-use transitions, such as the conversion of grasslands to croplands, have been shown to reduce soil organic carbon (SOC) stocks across Europe[26]. Vegetation cover plays a vital role in stabilizing soils and maintaining soil structure[27]. The removal or alteration of vegetation cover, especially woodland in past centuries, has exposed soils to increased erosion risks and nutrient losses[28,29]. Additionally, agricultural management practices (e.g., intensive fertilizer use or improper crop cultivation) can further affect soil vulnerability that leads to degradation[30,31]. However, certain land-use transitions can also generate positive outcomes. Throughout the last 25 years, substantial efforts have been undertaken toward forest restoration, leading to a 5.5% increase in forest cover (8.3 million hectares) across Europe[32]. Practices such as reforestation and the implementation of cover crops have demonstrated success in enhancing soil health and resilience[33,34].

[1]Institute of Geo-Hydroinformatics, Hamburg University of Technology, Hamburg, Germany. [2]United Nations University Hub on Engineering to Face Climate Change at the Hamburg University of Technology, United Nations University Institute for Water, Environment and Health (UNU-INWEH), Hamburg, Germany. [3]The Climate and Environmental Research Institute NILU, Kjeller, Norway. [4]Department of Environmental Sciences, Environmental Geosciences, University of Basel, Basel, Switzerland. [5]European Commission, Joint Research Centre (JRC), Ispra, Italy. [6]UK Centre for Ecology & Hydrology, Bangor, UK. [7]Department of Civil and Environmental Engineering, University of Nevada, Reno, NV, USA. ✉e-mail: mehdi.afshar@tuhh.de; nima.shokri@tuhh.de

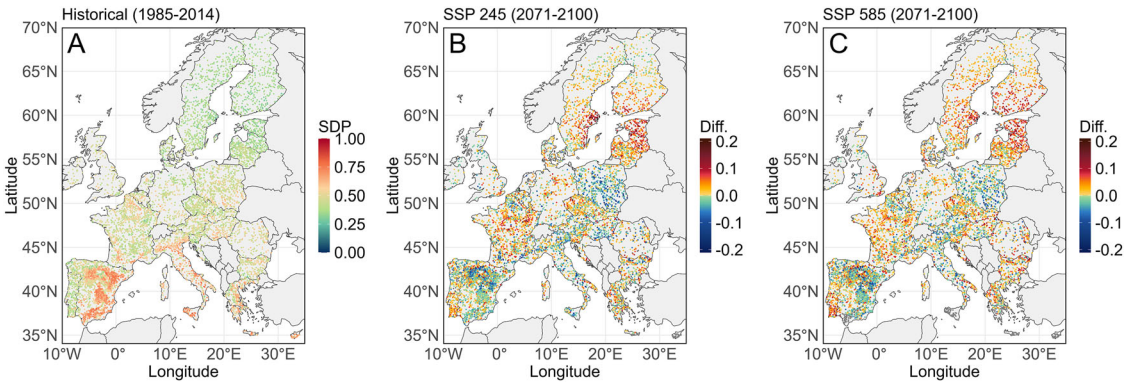

Fig. 1 | Spatial distribution and projected changes in SDP (soil degradation proxy) across Europe. Each symbol represents a LUCAS sampling point. **A** Map of the historical SDP across Europe based on LUCAS observations, **B** projected change in SDP (future minus historical) under the SSP2-4.5 scenario for the far-future (2071–2100), **C** projected change in SDP under the SSP5-8.5 scenario for the far-future (2071–2100). Dark gray colors denote locations excluded due to extrapolation beyond the training domain.

The combined impact of land-use and climate change can intensify soil degradation in many regions[23,35], yet in some settings, land-use transitions and restoration can partially offset climate pressure. Together, these dynamics can either amplify or mitigate vulnerability depending on local conditions, trajectories, and management. Addressing soil degradation, driven by changes in land-use and climate, requires an understanding of interactions between these drivers and soil health conditions across environmental and socioecological contexts[36]. Understanding the current state of soil degradation is essential for anticipating how climate and land-use pressures will shape future soil vulnerability[37,38].

Assessing climate change impacts on soil degradation faces several key challenges. The uncertainty in climate and socioeconomic projections introduces significant variability in the predicted outcomes for soil degradation processes[20,39], making it hard to produce reliable estimates for soil degradation susceptibility under different potential emission conditions. The quality and resolution of field observation data, as well as the definition of soil degradation proxy (SDP), play a key role in such types of analysis[14,38,40,41]. Additionally, the interaction between natural and human factors, such as land-use and agricultural practices, adds further complexity to the model predictions and limits the current prediction models to capture local differences in soil conditions (e.g., land management) for different regions[42–44].

The SDP[38] is developed as a response to the need for an integrated, balanced approach to assess the relative vulnerability of soil to degradation (Supplementary Material 1). The SDP combines four key indicators of soil erosion rate, electrical conductivity (EC), soil pH, and SOC with equal weights to represent the physical, chemical, and biological aspects of soil degradation (see "Methods"). The SDP provides a continuous and relative measure of vulnerability to degradation, designed to evaluate the soil status at a given location in relation to its past or potential future conditions, not as an absolute measure of the current soil state. Differences in SDP values may also reflect natural variations in soil and environmental properties that are not necessarily linked to human activity.

The current relative vulnerability state of soils has been evaluated using the SDP, revealing that land-use change, management practices, and climate factors play important roles in shaping the susceptibility to degradation across different soil types[38]. However, few studies have explored how these dynamics might evolve under future climate and land-use fraction change scenarios. Current studies have mostly focused on specific soil degradation processes, such as soil erosion[20] or salinization[39], without offering a comprehensive and holistic assessment of how future climate change and land-use transitions might impact overall soil functioning. Hence, the broader understanding of future soil vulnerability to degradation under combined pressures of climate and land-use change remains largely unexplored.

This study addresses current gaps in understanding how the combined impacts of climate change and land-use transition influence the relative vulnerability of soil to degradation across Europe. By integrating climate projections with land-use scenarios, we assess how environmental drivers interact to shape soil susceptibility to degradation across the land-use/cover area frame survey observations (LUCAS)[45–48]. We use a machine learning modeling approach (i.e., random forest; RF) to predict the relative vulnerability of soil to degradation under different shared socioeconomic pathways (SSP2-4.5 and SSP5-8.5) for both near-future (2031–2060) and far-future (2071–2100) periods. Through this quantitative assessment of future soil vulnerability, we identify the main covariates governing projected changes and the key drivers of soil degradation, thereby providing insights for sustainable land management strategies and climate change mitigation efforts.

Spatial patterns of soil degradation proxy in Europe

The spatial distribution of the SDP across Europe under historical conditions (i.e., between years 1985 and 2014) reveals regional patterns in relative vulnerability of soil to degradation (Fig. 1A). Mineral soils with lower SDP values, indicating more resilient soil conditions, are predominantly located in the northern regions of Europe (shown in dark blue). Countries, such as Estonia and Finland, exhibit some of the lowest SDP values, averaging 0.34 and 0.35, respectively. In contrast, higher SDP values, shown in dark red, are concentrated in southern Europe, particularly in Cyprus, Spain, and Italy (with average historical SDP values of 0.66, 0.60, and 0.59, respectively). Across sites, the historical distribution has an interquartile range of 0.16 and a ninetieth-percentile level of 0.68.

We observed a northeast-to-southwest gradient in the SDP distribution[37]. However, part of this north-south contrast reflects climatic erosivity and relief that are embedded in the erosion component, which implies that higher erosion scores in the south do not by themselves represent poorer management. Meanwhile, natural gradients in soil processes also contribute to regional contrasts in SDP, as inherent soil characteristics can lead to higher or lower index values even under undisturbed conditions. These natural differences, however, may further amplify vulnerability in certain regions when combined with anthropogenic pressures.

Projected changes in SDP under future land-use and climate scenarios are presented in Fig. 1B (SSP2-4.5), 1C (SSP5-8.5) for the far-future (near-future and their uncertainty level maps are also mapped in Figs. S1 and S2, respectively). The associated uncertainty varies across space, reflecting differences among annual land-use trajectories (Fig. S3), climate models (Fig. S4), and model limitations. Under the SSP2-4.5 scenario for the near-future (2031–2060), slight increases in SDP are projected for many of the LUCAS observations. Under both scenarios, northern Europe exhibits higher SDP changes relative to the historical baseline, and SSP5-8.5

generally exceeds SSP2-4.5 (Fig. S1H), indicating stronger climate pressure toward the end of the century. For instance, Estonia and Latvia show average SDP increases of +0.07 (+20.3% above their historical value) and +0.05 (+14.4% above their historical value), respectively, with marginal differences in the higher emission SSP5-8.5 scenario (Fig. 1B, C). Overall, the late-century period shows the greatest uncertainty among the model results for both scenarios. This means that the larger changes in SDP during this time are partly due to higher uncertainty in that period, rather than the effects of the scenarios themselves (Fig. S1H). It is also noteworthy here that these changes represent movement on a standardized index and are interpreted relative to historical distribution, not as a metric of distance or probabilities.

Conversely, several countries in southern and central Europe show a slight decreasing trend in SDP under future land-use and climate scenarios, indicating potential improvements in soil conditions. Poland and Spain, for example, show average SDP changes of −0.034 (−7.3%) and −0.013 (−2.2%), respectively, under SSP2-4.5 (Fig. 1B), with comparable results under the higher-emission SSP5-8.5 scenario (Fig. 1C). Our analysis indicates that these relatively small reductions are mainly linked to projected shifts in land-use composition, particularly the decline in cropland fractions and the corresponding expansion of secondary vegetation types (e.g., shrubs and grasslands; Fig. S3). These transitions likely restore SOC and stabilize pH levels closer to neutral conditions by reducing fertilizer and lime inputs, accumulating organic matter, and enhancing natural leaching processes.

Overall, both future scenarios yield broadly similar spatial patterns and magnitudes of change in SDP. The relatively small differences between SSP2-4.5 and SSP5-8.5 are consistent with findings that scenario trajectories diverge more substantially toward the end of the century[49–51]. Moreover, machine-learning models, such as random forests, tend to represent responses within the range of learned relationships, which can lead to nonlinear or saturating behavior in projected SDP changes under stronger climatic forcing. To ensure robust late-century projections, we explicitly masked predictions associated with combinations of climate and land-use predictors that fall outside the training-domain bounds, thereby avoiding extrapolation-related biases. On average across climate models, this masking affected approximately 5–6% of locations under near-future conditions (2031–2060), increasing to about 8% under SSP2-4.5 and 15% under SSP5-8.5 by the end of the century (2071–2100). Analysis of the variation in SSP-driven differences across climate models (Supplementary Figs. S5 and S6) further indicates that SSP5-8.5 produces higher SDP values than SSP2-4.5 for approximately 65% of locations, while a smaller but non-negligible fraction exhibits lower SDP under SSP5-8.5. These cases are primarily associated with land-use transitions, where projected conversions of croplands to shrublands and grasslands offset climate-driven increases in SDP despite higher temperatures.

Model performance and influential factors

The RF models reproduced historical spatial variation in SDP with median R-squared of ~0.58 and mean squared error (MSE) of ~0.009 across the 18 climate models, based on validation using 30% of the data. Variable importance analysis highlights that both land-use and climate variables play key roles in determining SDP, with temperate deciduous trees (Tedt), near-surface air temperature (TA), evergreen coniferous trees (Ect), precipitation (PR), and soil clay fraction (CLY) among the top contributors. Full diagnostics and relative importance of other variables are provided in Fig. S1.

Indicator-level contributions to SDP across Europe

By projecting each SDP component across both near (2031–2060) and far (2071–2100) future periods, we identified the underlying biochemical and physical processes that govern the changes in SDP under future climate and land-use trajectories (Fig. 2 and Figs. S7–S11). In the far-future, increases in SDP were primarily linked to declines in SOC, along with elevated erosion rates and rising EC, whereas decreases were most often associated with pH moving toward neutrality in previously alkaline settings (Fig. 2A, B).

The spatial maps of the dominant indicator (Fig. 2A, B) show that under both scenarios in northern and central Europe, increments in SDP are mainly governed by SOC and erosion rates, whereas pH-related decreases are more common in parts of the Mediterranean basin. The stacked frequencies (Fig. 2C, D) also confirm these patterns. Over forested systems and cold-climate zones, changes in SDP are dominated by SOC- and erosion-driven increases, while over croplands and arid zones, pH-related decreases dominate.

Under the SSP2-4.5 scenario, 12.05%, 12%, and 9.81% of observation sites account for increases in SDP governed by a decrease in SOC, an increase in EC, and an erosion rate, respectively. Under SSP5-8.5, these values change to 14.72%, 10.79%, and 11.03%, respectively (Fig. 2C, D). The frequency of decreases in SDP associated with pH normalization changes little between scenarios, from 18.6% of the sites under SSP2-4.5 to 16.7% of the sites under SSP5-8.5 scenarios. Although the overall spatial patterns are similar, there are small differences between the two scenarios. Part of the scenario differences stems from sites that shift from stable or decreasing SDP under SSP2-4.5 to increasing SDP under SSP5-8.5, reflecting a broader intensification of degradation risk. Differences also emerge where two indicators contribute nearly equally; a small additional climate shift can tip the balance and change which process appears dominant. In eastern Sweden, for example, EC is dominant under SSP2-4.5, whereas under SSP5-8.5 the erosion contribution becomes dominant. Overall, an integrated assessment of all indicators reveals a gradual shift toward more adverse soil conditions, especially in far-future scenarios. Although some localized improvements, primarily governed by pH normalization and reductions in EC, are evident, losses in SOC and increased erosion rate remain the main components shaping soil degradation at the continental scale (Fig. S7E–H).

Drivers of changes in the relative vulnerability of soil to degradation

Our analysis of the primary drivers causing changes in the SDP under future scenarios shows that although the relative dominance of drivers varies across space and time, SDP decrements are generally associated with land-use change, whereas increments in SDP are primarily associated with climate change (Fig. 3 and Figs. S12–S15). For example, in Poland, land-use changes would be the predominant factor contributing to the estimated reductions in SDP, with 63% and 53.1% of LUCAS points over it falling in this category under SSP2-4.5 and SSP 5-8.5 scenarios, respectively (Fig. S13).

Conversely, increases in SDP are associated mainly with climate-related factors that are prevalent in northern European countries. In Estonia, for example, 93% and 94% of observation points are projected to experience climate-induced rises in SDP under the SSP2-4.5 and SSP5-8.5 scenarios in the far-future, respectively. The projected intensification of precipitation events (Fig. S4) is expected to elevate soil erosivity at higher latitudes, while warming temperatures may accelerate organic matter decomposition, leading to reductions in SOC stocks (Fig. 2). Together, these processes, sometimes compounded by adverse land-use changes, such as deforestation, contribute to a higher rise in SDP in these regions under future climate and land-use scenarios.

Comparing the far-future outcomes of SSP5-8.5 with SSP2-4.5, the maps and frequencies of SDP change drivers show a continental shift toward climate-driven increases in SDP (Fig. 3C, D). The joint probability between the dominant drivers of SDP change (climate, land-use, or both) and the governing SDP components further summarizes these relationships across scenarios and time periods (Fig. S16). Climate change-driven increases in SDP (shown with orange color) expand across the Nordic and Baltic regions and into central Europe, while land-use driven decreases (shown with light blue) become more localized around parts of the Mediterranean and central Europe. This shift is already visible by mid-century (although marginal) with SSP5-8.5 showing a larger share of climate-driven increases than SSP2-4.5 (1540 sites in Fig. S12E vs. 2032 sites in Fig. S12G), and it strengthens by late century with higher climate-driven shares under SSP5-8.5 than SSP2-4.5 (1522 sites in Fig. 3C vs. 2950 sites in Fig. 3D).

Analysis of the relative frequencies across different land-use and climate types (Fig. 3E, F) shows that in arid zones, land-use-driven declines in SDP are particularly prominent under the SSP2-4.5 scenario, accounting for

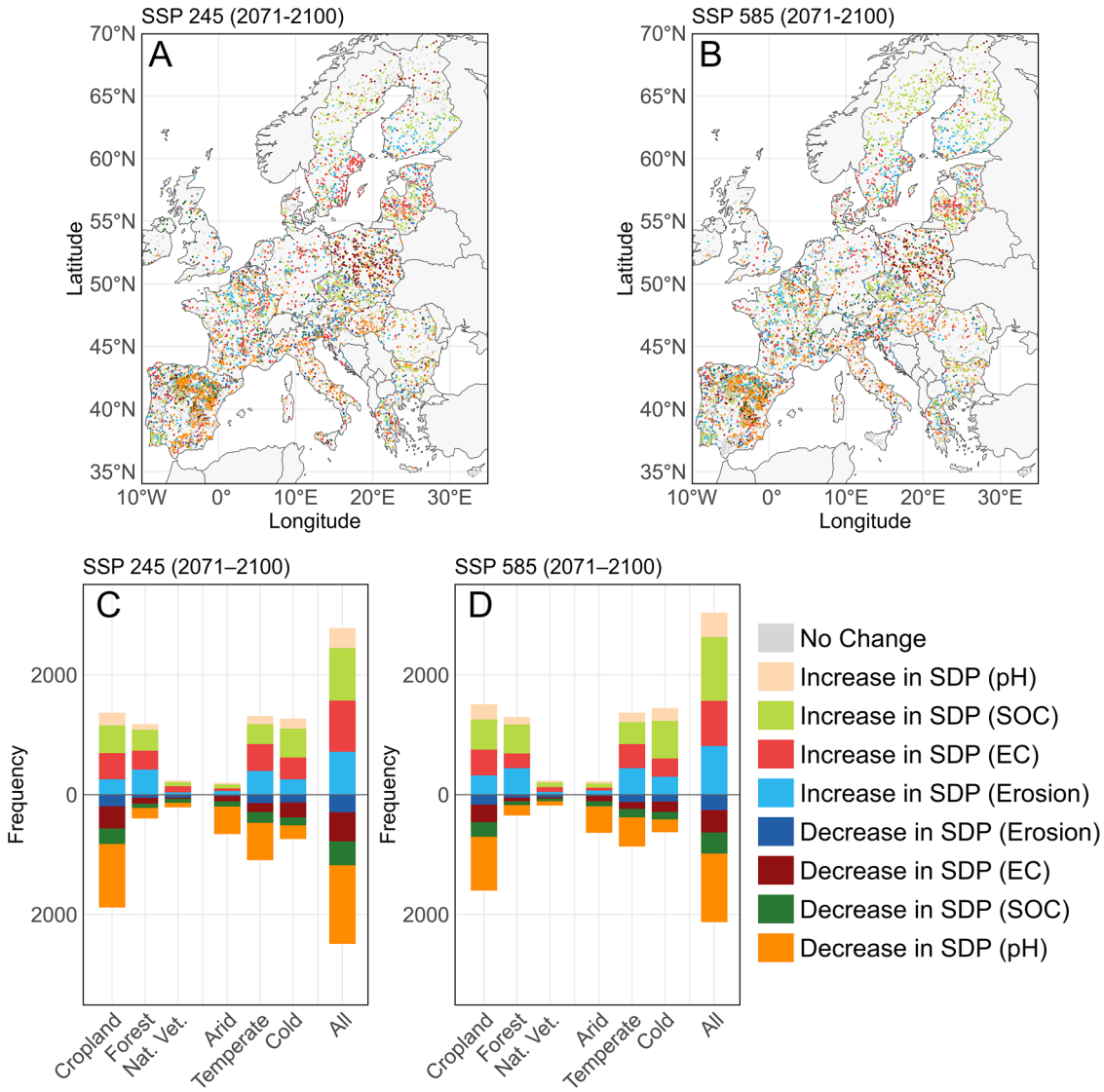

Fig. 2 | Dominant indicators governing changes in the SDP across Europe under future climate and land-use scenarios. Each symbol represents a LUCAS sampling point. **A**, **B** Maps showing the dominant SDP indicator (erosion, EC, SOC, and pH). **A** SSP2-4.5 far-future (2071–2100), **B** SSP5-8.5 far-future (2071–2100). **C**, **D** Frequency of change types for each indicator grouped by land-use and climate zones under the considered scenario-time combinations. **C** SSP2-4.5 far-future, **D** SSP5-8.5 far-future. Indicator changes are categorized based on relative increases or decreases in SDP and mapped to corresponding environmental settings. Gray colors denote locations excluded due to extrapolation beyond the training domain.

29.5% of sites. Under SSP5-8.5, this share declines to 24.9%, reflecting stronger late-century climate pressure. Yet the persistence of a measurable fraction of land-use-driven decreases under the high-emission scenario indicates that land management remains as a meaningful strategy to prevent degradation and potential desertification.

Forests emerge as hotspots of climate-driven vulnerability in both scenarios. Across Europe, the majority of forest sites show increases in SDP attributable to climate pressures under SSP2-4.5, and this share grows further under SSP5-8.5. For example, climate-driven increases affect about 32.2% of forest sites, rising to 54.9% under the high-emission pathway (SSP5-8.5). These increases are consistent with intensified precipitation events, which heighten erosivity, and with warming conditions that accelerate organic matter decomposition. This predicted loss of SOC in high latitude carbon-rich soils is consistent with experimental evidence[52]. Both erosion and SOC loss often combine and contribute to soil degradation (Figs. 2C, D, and 3E, F). Changes in SDP values show that even in regions with stable land-use, climate change alone can substantially elevate soil vulnerability.

Discussion

The results of this study correspond closely with those of Prăvălie et al.[41] and Borrelli et al.[20], highlighting the substantial impact of concurrent land degradation processes and climate change on soil vulnerability in Europe. Borrelli et al.[20] projected considerable increases in global soil erosion driven by climate change-induced factors, consistent with our finding that under the SSP5-8.5 scenario, climate change markedly intensifies soil relative vulnerability through increased erosivity. Our projections also align with predictions from Panagos et al.[53], which suggest that soil erosion could rise by 13–25% across nearly 80% of the European Union[25]. Moreover, the mapping of multiple land degradation pathways shown by Prăvălie et al.[41] aligns with our historical SDP map, particularly in regions like southern Europe, where high SDP values coincide with hotspots of concurrent degradation processes. Although these correspondences cannot be considered a direct validation of our analyses and simulations, they provide reassurance that our relative vulnerability estimates are broadly consistent with independent datasets. However, while previous studies have mainly applied deterministic models of specific degradation types, our machine

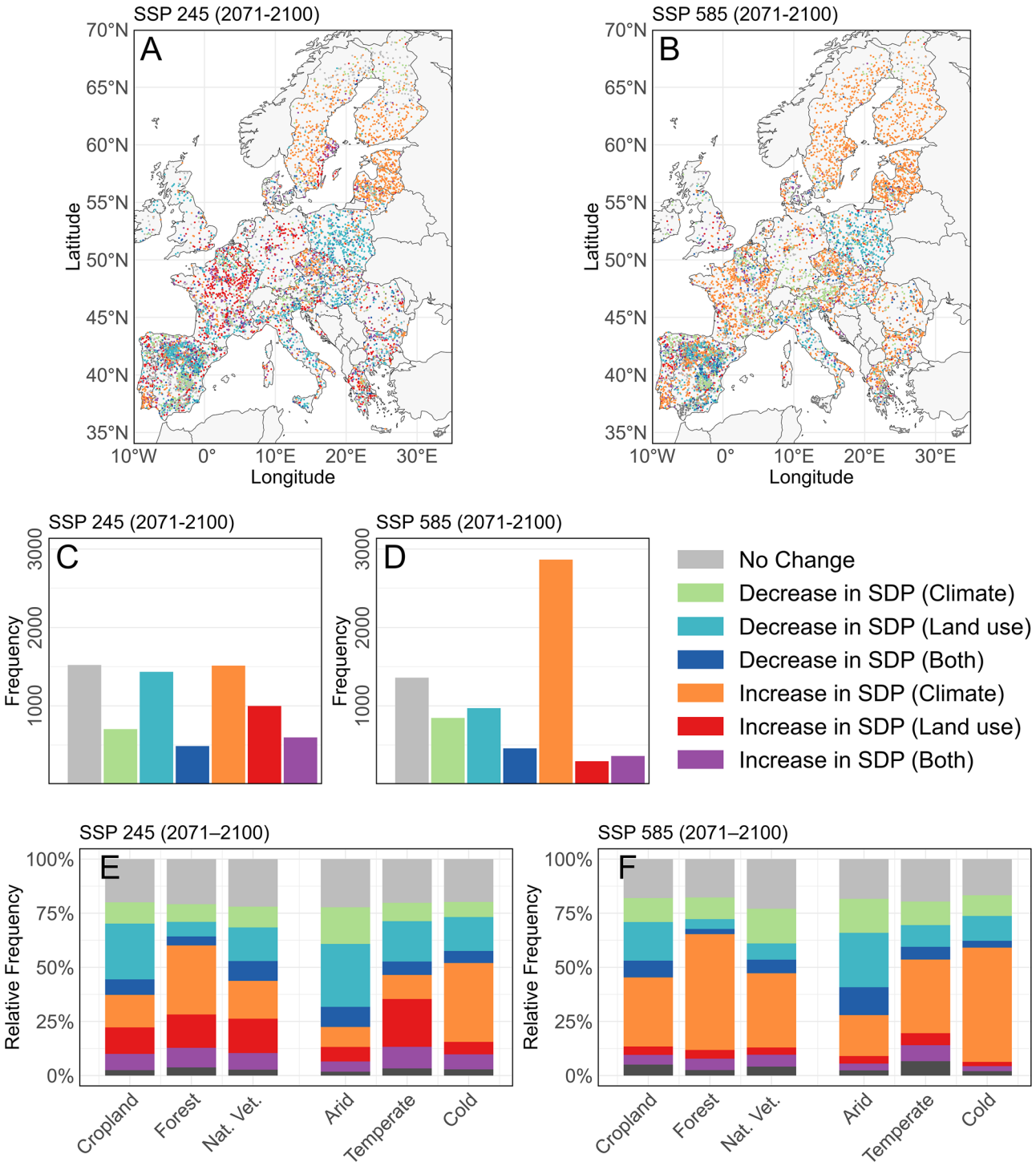

Fig. 3 | Drivers of changes in SDP (soil degradation proxy) across Europe under different climate and land-use scenarios. Each symbol represents a LUCAS sampling point. Maps illustrating the drivers of change under **A** SSP2-4.5 far-future (2071–2100), **B** SSP5-8.5 far-future (2071–2100). Frequency of LUCAS points in each change type for the considered scenarios: **C** SSP2-4.5 far-future, **D** SSP5-8.5 far-future. Relative frequencies of each change type across different land-use and climate types for the considered scenarios: **E** SSP2-4.5 far-future, **F** SSP5-8.5 far-future. Land-use types include cropland, forest, and natural vegetation. Climate types are arid, temperate, and cold. Change types are denoted as: no change, decrease in SDP due to climate, decrease in SDP due to land-use, decrease in SDP due to both, increase in SDP due to climate, increase in SDP due to land-use, increase in SDP due to both. Dark gray colors denote locations excluded due to extrapolation beyond the training domain.

learning framework provides a more flexible and integrative tool for simulating future soil relative vulnerability under diverse climate and land-use scenarios.

Different studies have shown that climate change could intensify pressures on agricultural production and stability[54–56]. According to the LUCAS LUC (land-use and climate across scales land-use and land cover change) dataset[56,57], land-use projections used in this study, one adaptive response in southwestern Europe involves a reduction in cropland fractions. Although these datasets inherently carry uncertainties related to underlying model assumptions and socioeconomic pathways[58–60], such transitions can

lower the relative vulnerability of soils to degradation where cropland contraction allows secondary vegetation to establish and soil properties begin to recover[61]. However, our modeling framework is not designed to explicitly quantify the potential benefits of restorative practices. Future extensions could include explicit scenarios of positive land management interventions to evaluate their mitigating potential.

An important limitation of this study is associated with the representation of uncertainty in future land-use trajectories. In this study, climate uncertainty is explored through an ensemble of 18 global climate models, allowing us to capture a wide range of plausible future climate conditions. In contrast, land-use projections rely on a single harmonized modeling framework (LUCAS LUC), which provides SSP-consistent, annually resolved land-use fractions tailored for Europe. While this dataset represents one plausible and internally consistent land-use pathway, it does not capture structural land-use uncertainty arising from alternative land-system model assumptions, socioeconomic narratives, or policy pathways. Recent global analyses further indicate that European land-use trajectories are sensitive to broader socioeconomic and demand-side drivers, suggesting that alternative pathways beyond SSP-based business-as-usual assumptions are plausible[62]. As a result, uncertainty related to SDP predictions is represented asymmetrically in this study, with climate uncertainty sampled more extensively than land-use uncertainty. Hence, the projected soil vulnerability outcomes should be interpreted as conditional on the assumed land-use trajectory. This asymmetry reflects the current lack of a structural land-use ensemble for Europe that provides the spatial resolution and temporal continuity required for this analysis. Incorporating ensembles of alternative European land-use models, therefore, remains an important priority for future research as such data become available.

Increasing soil vulnerability poses a significant threat to SDG 2 (zero hunger) by undermining food security in regions facing intensified degradation pressures. Declining soil quality can reduce agricultural productivity, threaten the livelihoods of farming communities, and exacerbate economic instability in areas heavily reliant on agricultural production. The climate-driven intensification of soil degradation also intersects with the objectives of SDG 13 (climate action), emphasizing the urgency of robust mitigation and adaptation strategies to protect soil-based ecosystems. Furthermore, this research supports SDG 15 (life on land) by highlighting the role of sustainable land management in reducing degradation risks and restoring degraded soils. By identifying the key drivers of soil degradation and mapping vulnerable regions under both current and future scenarios, our study provides actionable insights to guide integrated policy responses aimed at ensuring the long-term resilience and functionality of European soils and their ability to adapt and transition under changing climate conditions.

The SDP provides a relative, composite measure of soil vulnerability that integrates four degradation-related indicators (SOC, erosion rate, EC, and pH). Increases in SDP in specific regions can therefore be linked to underlying drivers (e.g., SOC losses, higher erosion rates, or increasing salinity). However, our framework does not explicitly quantify the rate at which these processes occur. Thus, the results should not be read as direct measurements of degradation rates, nor as maps of historical, present, and future time periods' degradation status.

Moreover, the spatial patterns of SDP partly reflect inherent soil property variability. Some deviations from reference conditions may arise from natural pedogenic differences rather than human-induced change. For example, a naturally acidic soil in a cool, forested landscape and a sandy, alkaline soil in a dry grassland may have very different SDP values despite both being in undisturbed, natural conditions. Such differences reflect inherent soil and environmental properties and may not necessarily indicate human-induced degradation. Given that the RF framework is trained on large-scale covariate relationships, the projections represent empirical associations at continental resolution and do not explicitly resolve the underlying soil-forming mechanisms operating at local scales. Hence, relationships learned in one pedo-climatic domain may not be mechanistically transferable to other domains under altered climate regimes.

Although the SDP components are evaluated separately for attribution purposes, soil degradation processes can interact in coupled and nonlinear ways (e.g., erosion-induced SOC depletion), and their explicit representation remained limited within the current continental-scale modeling framework.

SDP is a standardized and unitless index that is interpreted relative to the historical distribution, and it does not diagnose a single process or attribute a cause where specific driver data are not available. The likelihood of individual pressures, such as erosion, salinization, acidification, and SOC loss, is not uniform across soils or pedo-climatic zones, so interpretation should consider soil context. Future work could improve the approach by calibrating reference ranges within specific soil types or biogeographic units. The LUCAS sample used here is dominated by mineral soils, so the reported gradients primarily reflect mineral soil behavior.

It is important to acknowledge that the effectiveness of the SDP in capturing the relative vulnerability of soil to degradation depends significantly on both the number of samples and the diversity of indicators incorporated into its calculation[38]. For example, we cannot fully separate natural susceptibility from management effects with the available predictors. Higher erosion propensity in Mediterranean settings may arise from climate and relief as well as land-use. For this reason, we interpret SDP as relative vulnerability, and we avoid using it as proof of mismanagement. Alongside these conceptual limits, although the RF models showed R-squared and MSE values comparable to those reported in other continental-scale soil modeling studies[39,63], a portion of the slight under-prediction of SDP values in historically vulnerable regions may result from the tendency of machine learning models to smooth out extremes toward the mean and the inability to extrapolate reliably to environmental conditions that fall outside the range represented in the training data[64].

To minimize misinterpretation from such effects, we evaluated future projections relative to historically modeled SDP values instead of raw observations. Furthermore, comparisons between decomposed-driver experiments (when one of the land-use or climate variables remains at its historical level) and the full scenario (when both land-use and climate variables change) simulations indicate that in arid regions, SDP values tend to remain unchanged or increase when present-day land-use remains constant (Figs. S14 and S15). Therefore, observed reductions in SDP under combined scenarios are largely attributable to projected land-use transitions.

Results from statistical and process models can vary with reasonable changes in model structure, hyperparameters, or training data. Our projections rely on one learning algorithm (RF) and one harmonized set of predictors, so alternative choices could shift local values in our predictions. We reduced this sensitivity by using 18 different climate models, considering annual land-use realizations within each period, and reporting their ensemble uncertainty. However, even with these steps, some dependence on model structure and data might remain in our analysis. Future work can test stability through multi-algorithm ensembles, predictor knock-out or replacement experiments, and bootstrap resampling across training sites. Accordingly, the maps and statistics presented here should be read as decision-support evidence that highlights relative patterns under the stated assumptions and should not be interpreted as a single definitive depiction of future relative vulnerability of soil to degradation.

Another limitation of this study is related to the absence of harmonized, continent-wide observations of soil degradation intensity that could serve as a direct validation target. Yet the SDP framework can be externally evaluated with independent evidence. Spatial cross validations can compare high-SDP areas with vulnerable locations with EU reporting on soil threats. Temporal checks can back-cast and forward-test across other LUCAS surveys to test the reproducibility of spatial patterns and the sign of change. Component-level checks can also compare SOC, pH, EC, and erosion projections with independent monitoring, such as national soil inventories or sediment and runoff observations. Moreover, driver attribution can be examined by matching modeled land-abandonment signals with other simulated land-cover transitions from other pan-European maps[65–67].

Future research could enhance the predictive power and accuracy of SDP projections by incorporating a broader range of indicators. In this study, we adopted an equal weighting scheme, assigning equal weight to each of the four selected indicators. Future work could explore alternative weighting strategies to reflect the relative importance of specific degradation processes. Moreover, expanding the range of scenarios to include additional emission pathways and land-use trajectories would further increase the robustness of model projections, providing policymakers with a more comprehensive and adaptable tool for developing targeted soil conservation strategies at the continental scale.

Concluding remarks

In this study, a comprehensive assessment of the relative vulnerability of soil to degradation across Europe was conducted by integrating future climate change and land-use scenarios within a machine learning framework. Utilizing the SDP, we evaluated how projected conditions under two SSPs (SSP2-4.5 and SSP5-8.5) for the near-future (2031–2060) and far-future (2071–2100) are likely to influence soil condition and degradation risk.

Our findings highlight the critical importance of tailored soil conservation strategies that consider both land-use and climate change adaptation. While negative climate impacts in cold and forested regions are projected to substantially accelerate degradation, timely land-use interventions in arid regions could yield notable improvements in soil resilience. By incorporating high-resolution observational data from initiatives, such as LUCAS, we demonstrate the need for policymakers and land managers to prioritize adaptive measures that mitigate the adverse effects of climate change while leveraging targeted land-use interventions to build a more sustainable future for soil ecosystems. Moreover, this work highlights opportunities for innovative approaches, such as adopting a strategic, continental-scale policy framework that transcends national boundaries, laying the groundwork for a more adaptive, resilient, and sustainable future for European soils.

Materials and methods

Relative vulnerability of soil to degradation

We assessed the relative vulnerability of soil to degradation using the SDP, a continuous metric that integrates four key indicators of soil erosion rate, pH, EC, and SOC, that together reflect both ongoing pressures (e.g., erosion) and the current condition of soils (e.g., SOC, EC, and pH). These indicators were selected to capture complementary physical[9,68], chemical[39,68], and biological[68,69] dimensions relevant to soil functioning. We acknowledge that some of these properties vary naturally between soil types and are not always a direct result of degradation processes. In the current formulation of SDP, each indicator is rescaled to a dimensionless range of [0, 1] (representing a unitless score on a percentile scale) and contributes equally to the overall SDP (weight 0.25; Supplementary Materials 1), consistent with composite-indicator best practice[70]. It is noteworthy here that currently, EU soil-health frameworks specify indicators but offer no harmonized guidance on their relative weighting at the continental scale. The adopted equal-weighting scheme therefore represents a transparent and reproducible baseline aligned with established methodological standards[70]. The continuous structure of SDP makes it practical for tracking the relative vulnerability of soils to degradation over time in response to climate change and land-use transitions within a holistic framework.

Historical and future evaluation of SDP

To evaluate the impact of climate change and land-use transition on soil vulnerability over time, we trained the machine-learning model using SDP values at LUCAS locations with a mid-year land-use snapshot (year 2000) and mean climate for the historical window. Climate variables were averaged over 1985–2014, and the resulting random forest (RF) models were applied to simulate SDP values for historical (1985–2014) and future conditions. We used 30-year means for climate predictors over 1985–2014 so that the predictor climatology is anchored to the 2015 observation year and consistent with the CMIP6 historical period[71]. For future projections, we held soil parent properties constant, including topography and texture, at their historical values, while incorporating climate and land-use data projected under two shared socioeconomic pathways (SSP2-4.5 and SSP5-8.5) across two time horizons of near-future (2031–2060) and far-future (2071–2100). For each future period, we generated annual simulations (30 per period) that update land-use fractions each year, for every climate model, to propagate land-use variability within the period. Additionally, we developed two separate scenarios to isolate the individual effects of climate change and land-use change on projected soil vulnerability.

Study area and data sources

Our study focuses on the European continent, covering the EU-27 countries and the United Kingdom, as covered by the LUCAS framework (Fig. S17). We used the LUCAS soil dataset to extract three of the four indicators used in the SDP calculation (i.e., soil pH, EC, and SOC). For soil erosion rate, we used values extracted from the revised universal soil loss equation for the year 2016[72].

Predictor variables

The predictor variables used to train the RF models were selected to balance process relevance with the requirement for consistent, spatially complete data across Europe, available for both historical and future scenarios (Supplementary Table 1). To achieve this, we combined variables that remain relatively stable over time, such as soil parent material (sand, silt, and clay ratios; extracted from SoilGrids)[73], and topographic features (digital elevation model and local terrain variability), with variables that change under scenarios, including land-use fractions, mean annual temperature (tas), total precipitation (pr), and surface soil moisture (mrsos) that together represent the energy input, water supply, and realized moisture state that govern different soil degradation processes (e.g., SOC turnover, rainfall erosivity, and salinization risk) at a continental scale. All LUCAS sites were treated as independent training instances and linked to gridded predictors by direct co-location, and for each LUCAS coordinate, predictor values were then extracted from the corresponding grid cell.

Other potentially relevant indicators, such as vegetation indices (NDVI) or drought indices (e.g., standardized precipitation index), were considered but not included because they are either not consistently available for future projections at the required spatial and temporal resolution or would require additional bias correction and methodological treatment that falls beyond the scope of this study. Furthermore, the observational data used to train the models were collected in 2015 and 2018, during which most measured values remained relatively stable, and short-term climate fluctuations could not be consistently captured. Hence, our modeling framework is designed in a way to represent the influence of gradual changes in mean climate and land-use on soil vulnerability and does not explicitly capture short-term extreme events.

Climate data used in this study were obtained from the Coupled Model Intercomparison Project Phase 6 (CMIP6)[74] and accessed via the Copernicus Climate Data Store (CDS). The used climatic variables (i.e., tas, pr, and mrsos) were averaged across three time periods of 1985–2014 (historical), 2031–2060 (near-future), and 2071–2100 (far-future), under two SSPs (SSP2-4.5 and SSP5-8.5). To ensure consistency across scenarios, we selected 18 climate models that were available for both historical and future periods (listed in Supplementary Table 2).

Land-use fraction data were sourced from the LUCAS LUC dataset (version 1.1 at a spatial resolution of 0.1°)[57], developed within the CORDEX Flagship Pilot Study LUCAS to provide high-resolution, annually resolved land-use trajectories for regional climate modeling consistent with CMIP6 downscaling. LUCAS LUC applies a land-use translator to land-use harmonization (LUH2) trajectories[75] to produce annual plant functional type (PFT) fractional cover maps from 1950 to 2100, based on a 2015 LANDMATE PFT reference map, ensuring temporally continuous land-use forcing over the EURO-CORDEX domain. It is noteworthy here that for future periods, we retained climate as a 30-year mean and allowed land-use to vary year by year. We paired the constant period climate fields with the

corresponding annual LUCAS LUC map for each year within 2031–2060 and within 2071–2100, generated one prediction per year at every LUCAS site, and then averaged the 30 yearly predictions to obtain the period value.

Machine learning approach

We used the RF algorithm to model the relationship between environmental variables and soil vulnerability. To ensure data consistency, we selected LUCAS observations that remained unchanged between 2015 and 2018 (with absolute change in SDP < 0.05), reducing the dataset from 16,579 to 7433 points. We applied this filter to align site responses with 30-year climate means, reducing the influence of short-term disturbances or measurement variability on a model designed to learn mean-state relationships. This filtering step excluded observations potentially influenced by transient factors, such as recent management interventions or vegetation loss, allowing the training data to reflect stable land and climate conditions.

Model training used the mid-year land-use snapshot (year 2000) with historical mean climate (1985–2014). The RF models were trained once on 1985–2014 using the considered predictors and the corresponding SDP values at LUCAS sites. Static predictors (soil texture and topography) were held fixed for all projections. For each scenario and time window, we assembled new predictor stacks by substituting scenario-specific climate means and land-use fractions while keeping static predictors unchanged, then scored the trained RF models to obtain site-level projections. We also used an ensemble modeling approach to capture the uncertainties associated with climate projections and model outputs. For each time period, climate model, and climate scenario, we generated 30 annual SDP predictions based on archived outputs from the CMIP6 climate models and evolving land-use fractions. Period means were then computed per model, and final projections were obtained by averaging across the 18 climate models, and uncertainty was summarized as the standard deviation across annual simulations and across models.

Model validation was performed on the historical period by using a 70–30% stratified split for training and validation, and model performance was evaluated using the MSE and the coefficient of determination (R-squared) between predicted and observed SDP values. Hyperparameters were optimized using a grid search approach. Moreover, to evaluate the relative influence of input variables, we analyzed the variable importance metrics produced by each RF model individually.

To identify the dominant soil degradation contributors governing changes in SDP, we developed separate RF models for each individual SDP component (i.e., erosion rate, EC, pH, and SOC) using a consistent set of predictor variables used in the prediction of SDP across 18 climate models. In RF models developed to predict SDP components, we used the same predictor set as in the main RF model developed to predict SDP and processed them identically. Predictors included soil parent material and texture from SoilGrids, topographic features from a DEM, land-use fractions from the LUCAS LUC dataset, and climate means of near-surface air temperature, precipitation, and surface soil moisture. Each model was calibrated and validated against observed values, and projections were made for historical (1985–2014) and future conditions under SSP2-4.5 and SSP5-8.5 for the near (2031–2060) and far (2071–2100) future. We then computed ensemble means of the projected changes in each indicator and compared them with changes in the overall SDP. The indicator with the largest absolute change in the same direction (i.e., sign) as the overall SDP trend was identified as the dominant contributor.

We also performed driver decomposition experiments to determine the respective roles of climate and land-use change in driving shifts in predicted SDP. This involved generating two additional sets of scenario-based projections, one isolating the effect of climate change by keeping land-use at historical levels, and the other isolating the effect of land-use change by keeping climate variables at their historical values. By comparing the changes under these isolated conditions with the combined scenario, we identified whether climate, land-use, or both were the primary drivers of the changes in SDP. We acknowledge that the land-use trajectories used in this study are themselves derived under SSP assumptions and are therefore not fully independent of the climate scenarios. Hence, the driver decomposition experiments should be interpreted as diagnostic comparisons within the shared scenario framework that help attribute relative influence, not as fully independent causal decompositions.

The primary driver was determined based on its relative contribution to the total change in SDP. If either climate or land-use alone accounted for more than 50% of the total change, it was identified as the dominant driver. In cases where both contributed significantly (i.e., each >50%), we compared their proximity to the total change. Specifically, if the absolute difference between the total change and the climate-only scenario was less than half the corresponding difference for the land-use-only scenario, climate change was identified as the dominant driver, and vice versa. If neither factor met these criteria and the total change was less than 0.01, we categorized the result as "no change." Otherwise, both factors were considered equally influential.

All analyses were conducted using the R statistical software environment. Model development was performed using the randomForest package, and stratified sampling and hyperparameter tuning were implemented with the caret package (see Supplementary Materials 2 for scripts and implementation details).

Data availability

The raw soil property data used in this study were obtained from the LUCAS 2015 and 2018 surveys, managed by the European Soil Data Center (ESDC) and the Joint Research Center (JRC) (available at https://esdac.jrc.ec.europa.eu/). Climate projections for the historical and future periods (SSP2-4.5 and SSP5-8.5) were retrieved from the CMIP6 archive via the Climate Data Store (CDS; available at https://cds.climate.copernicus.eu/). Land-use and land-cover projection data were obtained from the LUCAS LUC dataset. All processed datasets generated during this study, including the calculated SDP values, model input features, and the custom R scripts for data analysis and visualization, have been deposited in the Zenodo repository at https://doi.org/10.5281/zenodo.18894179. Any other data supporting the findings of this study are available from the corresponding authors upon request.

Received: 21 May 2025; Accepted: 18 March 2026;
Published online: 04 April 2026

References

1. IPBES. *The IPBES Assessment Report on Land Degradation and Restoration* (IPBES, 2018).
2. Shokri, N. et al. Rethinking global soil degradation: drivers, impacts, and solutions. *Rev. Geophys.* **63**, e2025RG000883 (2025).
3. Lehmann, J., Bossio, D. A. & Kögel-Knabner, I. The concept and future prospects of soil health. *Nat. Rev. Earth Environ.* **1**, 544–553 (2020).
4. Neuenkamp, L. et al. Comprehensive tools for ecological restoration of soils foster sustainable use and resilience of agricultural land. *Commun. Biol.* **7**, 1577 (2024).
5. Amelung, W., Bossio, D. & de Vries, W. Towards a global-scale soil climate mitigation strategy. *Nat. Commun.* **11**, 5427 (2020).
6. Kraamwinkel, C. T., Beaulieu, A., Dias, T. & Howison, R. A. Planetary limits to soil degradation. *Commun. Earth Environ.* **2**, 249 (2021).
7. Wall, D., Nielsen, U. & Six, J. Soil biodiversity and human health. *Nature* **528**, 69–76 (2015).
8. Wagg, C., Bender, S. F., Widmer, F. & Van Der Heijden, M. G. Soil biodiversity and soil community composition determine ecosystem multifunctionality. *Proc. Natl. Acad. Sci. USA.* **111**, 5266–5270 (2014).
9. Borrelli, P. et al. An assessment of the global impact of 21st century land use change on soil erosion. *Nat. Commun.* **8**, 1–13 (2017).
10. Montanarella, L. et al. *The Status of the World's Soil Resources* (Technical Summary) (FAO and ITPS, 2015).
11. Foley, J. A. et al. Global consequences of land use. *Science* **309**, 570–574 (2005).
12. Veldkamp, E., Schmidt, M., Powers, J. S. & Corre, M. D. Deforestation and reforestation impacts on soils in the tropics. *Nat. Rev. Earth Environ.* **1**, 590–605 (2020).

13. Lal, R. Anthropogenic influences on world soils and implications to global food security. *Adv. Agron.* **93**, 69–93 (2007).
14. Panagos, P., Borrelli, P., Jones, A. & Robinson, D. A. A 1 billion euro mission: a soil deal for Europe. *Eur. J. Soil Sci.* **75**, e13466 (2024).
15. Siebert, J. et al. The effects of drought and nutrient addition on soil organisms vary across taxonomic groups, but are constant across seasons. *Sci. Rep.* **9**, 639 (2019).
16. Jansson, J. K. & Hofmockel, K. S. Soil microbiomes and climate change. *Nat. Rev. Microbiol.* **18**, 35–46 (2020).
17. Sáez-Sandino, T. et al. Increasing numbers of global change stressors reduce soil carbon worldwide. *Nat. Clim. Change* **14**, 740–745 (2024).
18. García-Palacios, P. et al. Evidence for large microbial-mediated losses of soil carbon under anthropogenic warming. *Nat. Rev. Earth Environ.* **2**, 507–517 (2021).
19. Patel, K. F. et al. Soil texture and environmental conditions influence the biogeochemical responses of soils to drought and flooding. *Commun. Earth Environ.* **2**, 127 (2021).
20. Borrelli, P. et al. Land use and climate change impacts on global soil erosion by water (2015–2070). *Proc. Natl. Acad. Sci. USA.* **117**, 21994–22001 (2020).
21. Buscardo, E. et al. Effects of natural and experimental drought on soil fungi and biogeochemistry in an Amazon rain forest. *Commun. Earth Environ.* **2**, 55 (2021).
22. Wu, J. et al. Vegetation degradation impacts soil nutrients and enzyme activities in wet meadow on the Qinghai-Tibet Plateau. *Sci. Rep.* **10**, 21271 (2020).
23. Sünnemann, M. et al. Climate change and cropland management compromise soil integrity and multifunctionality. *Commun. Earth Environ.* **4**, 394 (2023).
24. Hou, Q., Ji, Z., Yang, H. & Yu, X. Impacts of climate change and human activities on different degraded grassland based on NDVI. *Sci. Rep.* **12**, 15918 (2022).
25. Roy, P. S. et al. Anthropogenic land use and land cover changes—a review on its environmental consequences and climate change. *J. Indian Soc. Remote Sens.* **50**, 1615–1640 (2022).
26. De Rosa, D. et al. Soil organic carbon stocks in European croplands and grasslands: how much have we lost in the past decade? *Glob. Change Biol.* **30**, e16992 (2024).
27. Durán, J. & Delgado-Baquerizo, M. Vegetation structure determines the spatial variability of soil biodiversity across biomes. *Sci. Rep.* **10**, 21500 (2020).
28. Durán Zuazo, V. H. & Rodríguez Pleguezuelo, C .R. Soil-erosion and runoff prevention by plant covers. A review. *Agron. Sustain. Dev.* **28**, 65–86 (2008).
29. Mohammad, A. G. & Adam, M. A. The impact of vegetative cover type on runoff and soil erosion under different land uses. *Catena* **81**, 97–103 (2010).
30. Hu, W. et al. Soil structural vulnerability: critical review and conceptual development. *Geoderma* **430**, 116346 (2023).
31. Liu, L., Zheng, X., Wei, X., Kai, Z. & Xu, Y. Excessive application of chemical fertilizer and organophosphorus pesticides induced total phosphorus loss from planting causing surface water eutrophication. *Sci. Rep.* **11**, 23015 (2021).
32. Eurostat. Forests, forestry and logging–Statistics Explained https://ec.europa.eu/eurostat/statistics-explained/index.php?title=Forests,_forestry_and_logging (2025).
33. Souza, V. S. et al. Cover crops enhance soil health, crop yield and resilience of tropical agroecosystem. *Field Crops Res.* **322**, 109755 (2025).
34. Jourgholami, M., Ghassemi, T. & Labelle, E. R. Soil physio-chemical and biological indicators to evaluate the restoration of compacted soil following reforestation. *Ecol. Indic.* **101**, 102–110 (2019).
35. Rothacker, L. et al. Impact of climate change and human activity on soil landscapes over the past 12,300 years. *Sci. Rep.* **8**, 247 (2018).
36. Barbosa, O. L. H. et al. in *Climate Change and Land: IPCC Special Report on Climate Change, Desertification, Land Degradation, Sustainable Land Management, Food Security, and Greenhouse Gas Fluxes in Terrestrial Ecosystems* (eds Shukla, P. R. et al.) 345–436 (Cambridge University Press, 2022).
37. Saljnikov, E. et al. Understanding soils: their functions, use and degradation. in *Advances in Understanding Soil Degradation,* 1–42 (Springer International Publishing, 2021).
38. Afshar, M. H. et al. Spatial and temporal assessment of soil degradation risk in Europe. *Sci. Rep.* **15**, 44636 (2025).
39. Hassani, A., Azapagic, A. & Shokri, N. Global predictions of primary soil salinization under changing climate in the 21st century. *Nat. Commun.* **12**, 6663 (2021).
40. Prăvălie, R. et al. Arable lands under the pressure of multiple land degradation processes. A global perspective. *Environ. Res.* **194**, 110697 (2021).
41. Prăvălie, R. et al. A unifying modelling of multiple land degradation pathways in Europe. *Nat. Commun.* **15**, 3862 (2024).
42. Lu, A. et al. Fuzzy logic modeling of land degradation in a Loess Plateau Watershed, China. *Remote Sens.* **14**, 4779 (2022).
43. Gianoli, F., Weynants, M. & Cherlet, M. Land degradation in the European Union—where does the evidence converge? *Land Degrad. Dev.* **34**, 2256–2275 (2023).
44. Panagos, P. et al. How the EU soil observatory is providing solid science for healthy soils. *Eur. J. Soil Sci.* **75**, e13507 (2024).
45. Jones, A., Fernandez-Ugalde, O. & Scarpa, S. *LUCAS 2015 Topsoil Survey*. *Presentation of Dataset and Results* https://doi.org/10.2760/616084 (2020).
46. Fernández-Ugalde, O., Ballabio, C., Lugato, E., Scarpa, S. & Jones, A. *Assessment of Changes in Topsoil Properties in LUCAS Samples between 2009/2012 and 2015 Surveys* https://doi.org/10.2760/5503 (2020).
47. Fernandez-Ugalde, O. et al. *LUCAS 2018 Soil Module. Presentation of Dataset and Results* https://doi.org/10.2760/215013 (2022).
48. Orgiazzi, A., Ballabio, C., Panagos, P., Jones, A. & Fernández-Ugalde, O. LUCAS soil, the largest expandable soil dataset for Europe: a review. *Eur. J. Soil Sci.* **69**, 140–153 (2018).
49. Meinshausen, M. et al. The shared socio-economic pathway (SSP) greenhouse gas concentrations and their extensions to 2500. *Geosci. Model Dev.* **13**, 3571–3605 (2020).
50. Tebaldi, C. et al. Climate model projections from the scenario model intercomparison project (ScenarioMIP) of CMIP6. *Earth Syst. Dyn.* **12**, 253–293 (2021).
51. Popp, A. et al. Land-use futures in the shared socio-economic pathways. *Glob. Environ. Change* **42**, 331–345 (2017).
52. Crowther, T. W. et al. Quantifying global soil carbon losses in response to warming. *Nature* **540**, 104–108 (2016).
53. Panagos, P. et al. Projections of soil loss by water erosion in Europe by 2050. *Environ. Sci. Policy* **124**, 380–392 (2021).
54. Lobell, D. B. et al. Prioritizing climate change adaptation needs for food security in 2030. *Science* **319**, 607–610 (2008).
55. Rezaei, E. E. et al. Climate change impacts on crop yields. *Nat. Rev. Earth Environ.* **4**, 831–846 (2023).
56. Abbass, K. et al. A review of the global climate change impacts, adaptation, and sustainable mitigation measures. *Environ. Sci. Pollut. Res.* **29**, 42539–42559 (2022).
57. Hoffmann, P., Reinhart, V., Asselin, O. & Rechid, D. LUCAS LUC historical/future land use and land cover change description and quality assessment (Version 1.1). *World Data Center for Climate (WDCC) at DKRZ* https://www.wdc-climate.de/ui/entry?acronym=LUC_info_v1.1 (2024).
58. Molina Bacca, E. J. et al. Future land-use pattern projections and their differences within the ISIMIP3b framework. *Earth Syst. Dyn.* **16**, 753–801 (2025).

59. Prestele, R. et al. Hotspots of uncertainty in land-use and land-cover change projections: a global-scale model comparison. *Glob. Change Biol.* **22**, 3967–3983 (2016).
60. Alexander, P. et al. Assessing uncertainties in land cover projections. *Glob. Change Biol.* **23**, 767–781 (2017).
61. Sobhi Gollo, V., Afshar, M. H., Or, D. & Shokri, N. Impacts of land use change on nutrient balance and greenhouse gas emissions: a regional perspective. *NPJ Sustain. Agric.* **3**, 1–7 (2025).
62. von Jeetze, P. et al. Conservation outcomes of dietary transitions across different values of nature. *Nat. Sustain.* **8**, 1130–1142 (2025).
63. Schillaci, C. et al. Empirical estimation of saturated soil-paste electrical conductivity in the EU using pedotransfer functions and quantile regression forests: a mapping approach based on LUCAS topsoil data. *Geoderma* **454**, 117199 (2025).
64. Hateffard, F., Steinbuch, L. & Heuvelink, G. B. M. Evaluating the extrapolation potential of random forest digital soil mapping. *Geoderma* **441**, 116740 (2024).
65. Brown, C., Seo, B. & Rounsevell, M. Societal breakdown as an emergent property of large-scale behavioural models of land use change. *Earth Syst. Dyn.* **10**, 809–845 (2019).
66. Dou, Y., Zagaria, C., O'Connor, L., Thuiller, W. & Verburg, P. H. Using the nature futures framework as a lens for developing plural land use scenarios for Europe for 2050. *Glob. Environ. Change* **83**, 102766 (2023).
67. Harrison, P. A. et al. Differences between low-end and high-end climate change impacts in Europe across multiple sectors. *Reg. Environ. Change* **19**, 695–709 (2019).
68. Obalum, S. E., Chibuike, G. U., Peth, S. & Ouyang, Y. Soil organic matter as sole indicator of soil degradation. *Environ. Monit. Assess.* **189**, 176 (2017).
69. Lebron, I. et al. Patterns and thresholds for soil pH across Europe in relation to soil health and degradation. *Catena* **260**, 109454 (2025).
70. Centre, J. R. *Handbook on Constructing Composite Indicators: Methodology and User Guide* (OECD Publishing, 2008).
71. Group, W. M. O. W. WMO guidelines on the calculation of climate normals https://library.wmo.int/records/item/55797-wmo-guidelines-on-the-calculation-of-climate-normals (2017).
72. Panagos, P. et al. A soil erosion indicator for supporting agricultural, environmental and climate policies in the European Union. *Remote Sens.* **12**, 1365 (2020).
73. Poggio, L. et al. SoilGrids 2.0: producing soil information for the globe with quantified spatial uncertainty. *Soil* **7**, 217–240 (2021).
74. Eyring, V. et al. Overview of the Coupled Model Intercomparison Project Phase 6 (CMIP6) experimental design and organization. *Geosci. Model Dev.* **9**, 1937–1958 (2016).
75. Hurtt, G. C. et al. Harmonization of global land-use change and management for the period 850-2100 (LUH2) for CMIP6. *Geosci. Model Dev. Discuss.* https://doi.org/10.5194/gmd-2019-360 (2020).

Acknowledgements

This research is part of the project AI4SoilHealth (accelerating collection and use of soil health information using AI technology to support the Soil Deal for Europe and EU Soil Observatory), to support the Soil Deal for Europe and EU Soil funded Horizon Europe (grant no. 101086179).

Author contributions

Conceptualization: M.H.A., A.H., P.B., P.P., D.A.R., D.O., and N.S., methodology: M.H.A., A.H., validation: M.H.A., A.H., P.B., P.P., D.A.R., D.O., and N.S., formal analysis: M.H.A., investigation: M.H.A., A.H., P.B., P.P., D.A.R., D.O., and N.S., data curation: M.H.A., A.H., writing-original draft: M.H.A., writing-review and editing: M.H.A., A.H., P.B., P.P., D.A.R., D.O., N.S., visualization: M.H.A., supervision: N.S., funding acquisition: N.S.

Funding

Open Access funding enabled and organized by Projekt DEAL.

Competing interests

The authors declare no competing interests.

Additional information

Supplementary information The online version contains Supplementary material available at https://doi.org/10.1038/s44458-026-00064-4.

Correspondence and requests for materials should be addressed to Mehdi H. Afshar or Nima Shokri.

Peer review information *Communications Sustainability* thanks Jetse J. Stoorvogel and the other anonymous reviewer(s) for their contribution to the peer review of this work. Primary handling editors: Somaparna Ghosh. A peer review file is available.